PHYSICAL REVIEW E **79**, 020801(R) (2009)

Parameters influencing diffusion dynamics of an adsorbed polymer chain

Nazish Hoda and Satish Kumar
Department of Chemical Engineering and Materials Science, University of Minnesota, Minneapolis, Minnesota 55455, USA
(Received 16 August 2008; published 3 February 2009)

Brownian dynamics simulations with hydrodynamic interaction (HI) are performed to study the effect of chain length on the diffusion of a polymer chain adsorbed onto flat surfaces. Bead-rod as well as bead-spring chains, with Hookean and finitely extensible nonlinear elastic (FENE) springs, are used to model the polymer chain, and the no-slip boundary condition for the solvent is incorporated exactly. Simulations for short chains ($N \leqslant 100$) predict that the translational diffusivity in the planar direction $D_{\|} \sim N^{-\nu}$, where N is the chain length, with $\nu \approx 0.75$ for bead-rod chains and bead-spring chains connected by stiff FENE springs and $\nu \approx 1$ for bead-spring chains connected by flexible FENE and Hookean springs. We find that near chemically homogeneous surfaces, the scaling exponent ν depends upon three factors: chain flexibility, strength of HI, and solvent quality. The ν value changes from 0.75 to 1 with either an increase in chain flexibility, a decrease in the strength of HI, or a decrease in solvent quality. However, near a chemically heterogeneous surface, ν is always 1.

DOI: 10.1103/PhysRevE.79.020801 PACS number(s): 82.35.Gh, 83.10.Rs, 83.80.Rs

Adsorbed polymers arise in practical applications involving thin polymeric films and polymeric nanocomposites [1,2]. Also, visualization experiments are performed by binding polymer molecules onto flat surfaces [3]. Understanding the dynamics of adsorbed polymer molecules is thus of great interest. Experimental studies suggest that for a polymer chain adsorbed onto a lipid bilayer, the translational diffusivity in the planar direction $D_{\|} \sim N^{-1}$, where N is the chain length [2–5]. On the other hand, Sukhishvili *et al.* found that $D_{\|} \sim N^{-3/2}$ for a polymer chain adsorbed onto a monolayer surface of condensed octadecyltriethoxysilane [6,7]. The physics that controls these scalings remains an active area of research.

Molecular simulations have proven valuable in addressing this issue. Two-dimensional (2D) molecular dynamics (MD) simulations with explicit solvent initially suggested a breakdown of dynamical scaling [8], but later it was found that dynamical scaling holds when finite-size effects are properly accounted for [9]. In this case, it is observed that $D_{\|}$ scales logarithmically with N; i.e., the effective scaling exponent is zero. Both 2D MD simulations without explicit solvent and 2D Monte Carlo simulations suggest that when a surface is decorated by impenetrable obstacles, $D_{\|} \sim N^{-3/2}$ at higher obstacle number density, whereas $D_{\|} \sim N^{-1}$ at lower obstacle number density [10,11]. Recent 3D dissipative particle dynamics simulations yield scalings consistent with these results [12]. Mukherji *et al.* performed 3D MD simulations with implicit solvent and without hydrodynamic interaction (HI) and reported that $D_{\|} \sim N^{-3/2}$ for a polymer chain adsorbed onto an atomically corrugated surface in good solvent [13]. Also, the diffusion dynamics was found to depend upon chain length, strength of the polymer-surface interaction, and solvent quality [13]. In the 3D studies described above, the surface was physically heterogeneous; i.e., the surface was either modeled by discrete atoms or was decorated with obstacles. Desai *et al.* performed 3D MD simulations with explicit solvent of a polymer chain adsorbed onto a physically homogeneous surface (ideally flat) [5]. It was reported that $D_{\|} \sim N^{-3/4}$ for a chemically homogeneous surface, whereas $D_{\|} \sim N^{-1}$ for a chemically heterogeneous surface.

In all of these 3D simulation studies, the no-slip boundary condition for the solvent at the adsorbing surface is not incorporated exactly (see, e.g., Ref. [14]), leaving ambiguous its role in controlling the scaling of the diffusivity. In this article, we perform Brownian dynamics (BD) simulations with HI to study the dynamics of an adsorbed polymer chain. Our simulations incorporate the no-slip boundary condition for the solvent exactly by using an analytical expression for the velocity field, which is obtained by solving the Stokes equation with no-slip boundary conditions. The simulations are also used to probe the roles of chain flexibility, strength of HI, and solvent quality in controlling the diffusivity scalings.

We have previously used BD simulations with HI to study the adsorption of a polyelectrolyte molecule onto uniformly charged and charged patterned surfaces in a simple shear flow [15,16]. In our model, the surface is located at $z=0$ and the polymer chain remains above the surface. The computational domain extends infinitely in the x, y, and z directions. Both bead-rod and bead-spring models are adopted to describe a polymer chain. In both models, the polymer chain is represented by N beads connected through $N-1$ connectors (either springs or rods). A force balance on each of the beads yields the following stochastic differential equation (dimensionless) in the case of bead-spring chains:

$$\mathbf{r} = \mathbf{r}^{old} + \left[\mathbf{u} + \mathbf{D} \cdot \mathbf{F} + \frac{\partial}{\partial \mathbf{r}} \cdot \mathbf{D} \right] dt + \sqrt{2}\mathbf{B} \cdot d\mathbf{w}, \qquad (1)$$

where $\mathbf{r}$ is the $3N$-dimensional vector of new bead positions, $\mathbf{r}^{old}$ is the vector of bead positions at the old time step, and $\mathbf{u}$ is the unperturbed solvent velocity. The non-Brownian non-hydrodynamic force is given by $\mathbf{F}$, dt is the time step used in the simulation, and $\mathbf{D}=\mathbf{B}\cdot\mathbf{B}^T$ is the diffusivity tensor, whose dimensions are $3N \times 3N$. The random displacement vector $d\mathbf{w}$ has a Gaussian distribution with zero mean and variance dt. In the case of the bead-rod model, the corresponding stochastic differential equation is much more complicated; it

as well as the simulation algorithm can be found in Refs. [15,17,18].

The diffusivity tensor $\mathbf{D}$ has 3×3 block components $\mathbf{D}_{ij}$, which are given by

$$\mathbf{D}_{ij} = \mathbf{\Omega}_{ij} + \delta_{ij}\mathbf{I}, \tag{2}$$

where $\mathbf{I}$ is the identity tensor, δ_{ij} is the Kronecker delta, and the HI tensor (hereupon referred to as the mobility tensor) $\mathbf{\Omega}_{ij}(\mathbf{r}_i,\mathbf{r}_j)$ relates the velocity perturbation at $\mathbf{r}_i$ to a point force at $\mathbf{r}_j$. We express $\mathbf{\Omega}_{ij}$ as [15,19]

$$\mathbf{\Omega}_{ij} = (1-\delta_{ij})\mathbf{\Omega}^{OB}(\mathbf{r}_i,\mathbf{r}_j) + \mathbf{\Omega}^{W}(\mathbf{r}_i,\mathbf{r}_j), \tag{3}$$

where $\mathbf{\Omega}^{OB}(\mathbf{r}_i,\mathbf{r}_j)$ is the Oseen-Burgers mobility tensor and $\mathbf{\Omega}^{W}(\mathbf{r}_i,\mathbf{r}_j)$ is a correction that accounts for the no-slip condition at a solid wall. In order to account for the finite bead-size in the simulations, $\mathbf{\Omega}^{OB}(\mathbf{r}_i,\mathbf{r}_j)$ is replaced by the Rotne-Prager-Yamakawa tensor [20,21] and $\mathbf{\Omega}^{W}(\mathbf{r}_i,\mathbf{r}_j)$ is taken as

$$\mathbf{\Omega}^{W}(\mathbf{r}_i,\mathbf{r}_j) = \mathbf{\Omega}^{W}_{PF}(\mathbf{r}_i,\mathbf{r}_j) - \frac{2a^2}{3}\mathbf{\Omega}^{W}_{c}(\mathbf{r}_i,\mathbf{r}_j), \tag{4}$$

where $\mathbf{\Omega}^{W}_{PF}(\mathbf{r}_i,\mathbf{r}_j)$ is the mobility tensor for Stokes flow due to a point force near a solid wall, the second term on the right-hand side is a correction term that accounts for finite bead size, and a is the hydrodynamic radius of the bead. The expressions for $\mathbf{\Omega}^{W}_{PF}(\mathbf{r}_i,\mathbf{r}_j)$ and $\mathbf{\Omega}^{W}_{c}(\mathbf{r}_i,\mathbf{r}_j)$ are given in Appendix B of Ref. [15].

The non-Brownian nonhydrodynamic forces on the ith bead are

$$\mathbf{F}_i = \mathbf{F}^{S}_i + \mathbf{F}^{LJ}_i + \mathbf{F}^{W}_i, \tag{5}$$

where $\mathbf{F}^{S}_i = \mathbf{F}^{S}(\mathbf{Q}_i) - \mathbf{F}^{S}(\mathbf{Q}_{i-1})$ is the spring force and $\mathbf{Q}_i = \mathbf{r}_{i+1} - \mathbf{r}_i$. In this study, we use both finitely extensible nonlinear elastic (FENE) and Hookean springs. The repulsive part of a Lennard-Jones potential, $\mathbf{F}^{LJ}_i$, accounts for excluded-volume interactions. As in our previous studies [15,16], bead-surface interactions $\mathbf{F}^{W}_i$, which confine the polymer chain to the surface, are modeled using a Lennard-Jones potential.

A time step of 10^{-4} is used in the simulations (the length and time scales used for nondimensionalization are given in the caption of Fig. 1). The properties of interest are obtained by averaging over the 24 different trajectories analyzed for a given set of parameters. Initial configurations corresponding to a Gaussian distribution of end-to-end distances are generated. A chain sampled from this distribution is placed at a distance $z=2.5$ above the surface, and we simulate the motion of a chain for 100–200 times the longest Rouse relaxation time. Runs were conducted on an IBM Bladecenter using a parallelized version of the code. To ensure that the chain remains adsorbed, we use an attractive potential of $15k_BT$, where k_B is Boltzmann's constant and T is the absolute temperature. For this potential value, the perpendicular component of the radius of gyration is less than 5% of the parallel component $R_{g\|}$, suggesting that the chain takes a pancakelike conformation. In order to study the dynamics of an adsorbed chain, we report $D_{\|}$. A 2D analog of the Einstein-Smoluchowski equation is used for calculating $D_{\|}$:

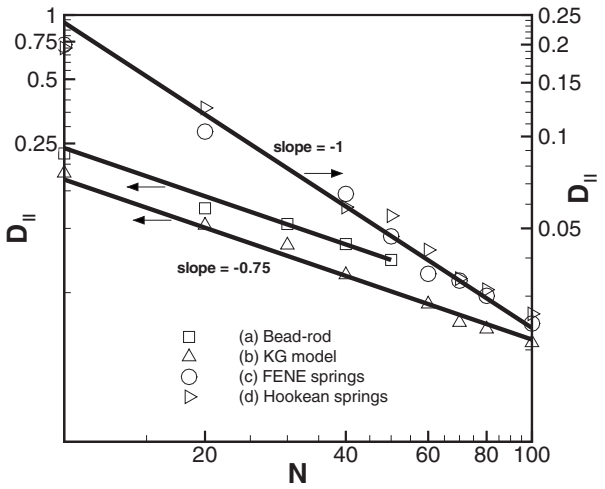

FIG. 1. Dependence of $D_{\|}$ on N. For bead-rod chains, the dimensionless excluded-volume diameter $d_{ev}=0.8$ and $a=0.5$, where the rod length l is used as the length scale. Note that decreasing d_{ev} decreases the range of excluded-volume repulsion; hence, this parameter controls the solvent quality. In the case of bead-spring chains, $\sqrt{k_BT/H}$ is used as the length scale for nondimensionalization, where H is the spring constant. We use $\zeta l^2/k_BT$ as the time scale for nondimensionalization. For the KG model, we use $a=d_{ev}/2=0.72$ and $b=HQ_0^2/k_BT=4.67$, where Q_0 is the maximum spring extension. We use $a=0.5$ and $d_{ev}=0.8$ in the cases of both Hookean and FENE springs and $b=56.25$ in the case of FENE springs.

$$D_{\|} = \langle \Delta r^2(t)\rangle/4t, \tag{6}$$

where the mean-square displacement of the center of mass of a chain, $\Delta r^2(t)$, is given by

$$\langle \Delta r^2(t)\rangle = \langle [\mathbf{r}_{c.m.}(t+\tau) - \mathbf{r}_{c.m.}(\tau)]^2\rangle, \tag{7}$$

where $\mathbf{r}_{c.m.}$ is the center of mass of the chain and τ is the time origin. The set of outer brackets denotes averaging over different time origins and the ensemble.

The effect of chain length on the diffusion of a polymer chain adsorbed onto a chemically homogeneous flat surface (hereupon referred to as smooth surface) is probed for a bead-rod chain and bead-spring chains connected by FENE or Hookean springs. We note that these results are for relatively short chains, as our computational resources only allowed investigation of values of $N\leqslant100$. For FENE springs, in one of the cases we use parameters similar to those used by Kremer and Grest [22] (KG model). Figure 1 shows the variation in $D_{\|}$ with N. We found that in all the cases, $R_{g\|}\sim N^{0.75}$ as adsorbed chains perform a 2D self-avoiding random walk [23]. For bead-rod chains and the KG model, $D_{\|}\sim N^{-0.75}$. According to the Stokes-Einstein formula, $D_{\|}\sim 1/R_{g\|}$, which implies that $D_{\|}\sim N^{-0.75}$ since $R_{g\|}\sim N^{0.75}$. The above results are thus consistent with the hydrodynamics of a sphere with hydrodynamic radius $R_{g\|}$ translating parallel to a planar surface [24], suggesting that HI is important; i.e., friction on the beads is correlated. On the other hand, $D_{\|}\sim N^{-1}$ for flexible FENE and Hookean springs, suggesting that friction on different segments of a polymer chain is uncorrelated. In order to understand the reasons for this depen-

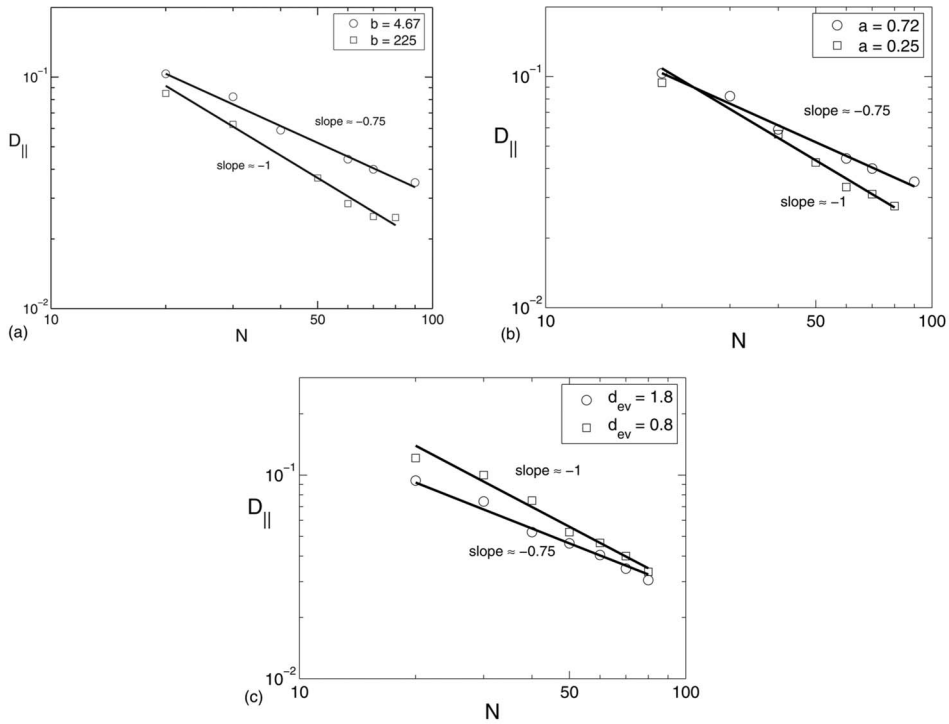

FIG. 2. Dependence of $D_{\|}$ on N for bead-spring chains connected by FENE springs (a) when b=4.67 and 225 and a=$d_{ev}/2$ =0.72, (b) when a=0.72 and 0.25, b=4.67, and d_{ev}=1.44, and (c) when d_{ev}=1.8 and 0.8, b=4.67, and a=0.9.

dence, we systematically probed the effects of chain flexibility b; strength of HI a; and solvent quality d_{ev}.

Figure 2 shows the dependence of $D_{\|}$ on N at different b, a, and d_{ev} values. It is clear from Fig. 2(a) that at small b, $D_{\|} \sim N^{-0.75}$, while at higher b, $D_{\|} \sim N^{-1}$, suggesting that HI is unimportant for flexible chains (higher b values). This is consistent with the notion that friction on different segments of a polymer chain is uncorrelated (HI is screened) in more flexible chains since beads are freer to move about. We also found that the scaling exponent changes from 0.75 to 1 with a decrease in a [cf. Fig. 2(b)]. It is noteworthy that the strength of HI is given by $(\zeta/\eta_s)\sqrt{H/(36\pi^3 k_B T)}(\propto a)$ [25], where ζ is the friction coefficient and η_s is the solvent viscosity. Since the HI strength weakens with a decrease in a, the correlation between friction on different segments of a polymer chain also weakens as a consequence. Figure 2(c) suggests that even a decrease in d_{ev} causes the scaling exponent to change from 0.75 to 1. A decrease in d_{ev} corresponds to a decrease in solvent quality. In poor solvent conditions, beads are freer to move closer to each other, reducing the correlation of friction on different segments of a polymer chain. Mukherji *et al.* also reported that polymer diffusivity near an atomically corrugated surface shows a stronger dependence on N under poor solvent conditions [13]. The above results suggest that both chain and solution properties affect the dynamics of a chain adsorbed onto a smooth surface.

To verify the above power-law dependence, we calculated the relaxation time of the end-to-end distance vector of an adsorbed chain, τ_R, and $R_{g\|}$. Table I shows the chain length dependence of τ_R, $R_{g\|}$, and $D_{\|}$ at different b, a, and d_{ev} values. The relaxation time follows three different scaling laws depending upon the values of b, a, and d_{ev}. In all cases, except for d_{ev}=0.8, $R_{g\|} \sim N^{0.75}$ as an adsorbed chain performs a 2D self-avoiding random walk under good solvent conditions (higher d_{ev}). For d_{ev}=0.8, a polymer chain forms a 2D globular structure (disklike); hence, $R_{g\|} \sim N^{0.5}$ [23]. In Table I, the chain length dependence of $D_{\|}$ is evaluated using the relation $D_{\|} \sim R_{g\|}^2/\tau_R$ [5]. Clearly, in all cases the N dependence of $D_{\|}$ listed in Table I and obtained independently from simulations (Fig. 2) is the same.

We also probed the scaling exponent near a chemically heterogeneous flat surface. In order to model bead-surface interaction near such a surface, we use the following potential [5]:

$$U(x,y,z) = U_{smooth}(z)\left[1 + \mathcal{A}\cos\left(\frac{2\pi x}{q}\right)\cos\left(\frac{2\pi y}{q}\right)\right], \quad (8)$$

where $U(x,y,z)$ and $U_{smooth}(z)$ are potentials near a chemically heterogeneous and smooth surface, respectively. The parameters $\mathcal{A}$ and q control the amplitude and wavelength of heterogeneity, and (x,y,z) is the bead coordinate. Figure 3 shows that $D_{\|} \sim N^{-1}$ for both the KG model and flexible FENE springs. This scaling is consistent with the fact that in the simulations, $\tau_R \sim N^{2.5}$ and $R_{g\|} \sim N^{0.75}$. The same scaling holds even at different $\mathcal{A}$ and q values. There is a higher probability of finding polymer segments in regions of stronger surface attraction, and the polymer segments resist moving to regions with weaker surface attraction. So surface friction is more dominant than HI near a chemically heterogeneous surface relative to a smooth surface. Hence the friction coefficient shows a stronger dependence on chain length.

In summary, our simulation results, which incorporate the no-slip boundary condition for the solvent exactly, suggest that both chain and solution properties affect the dynamics of a polymer chain adsorbed onto a flat surface. BD simulations predict that $D_{\|} \sim N^{-\nu}$, where ν can take two different values near a chemically homogeneous surface. We find that ν

TABLE I. Chain length dependence of τ_R, $R_{g\|}$, and $D_\|$ at different b values for $a=d_{ev}/2=0.72$, at different a values for $b=4.67$ and $d_{ev}=1.44$, and at different d_{ev} values for $b=4.67$ and $a=0.90$.

Effect of b			
b	τ_R	$R_{g\|}$	$D_\| \sim R_{g\|}^2/\tau_R$
4.67	$N^{2.25}$	$N^{0.75}$	$N^{-0.75}$
225	$N^{2.5}$	$N^{0.75}$	N^{-1}
Effect of a			
a	τ_R	$R_{g\|}$	$D_\| \sim R_{g\|}^2/\tau_R$
0.25	$N^{2.5}$	$N^{0.75}$	N^{-1}
0.72	$N^{2.25}$	$N^{0.75}$	$N^{-0.75}$
Effect of d_{ev}			
d_{ev}	τ_R	$R_{g\|}$	$D_\| \sim R_{g\|}^2/\tau_R$
0.80	N^2	$N^{0.5}$	N^{-1}
1.80	$N^{2.25}$	$N^{0.75}$	$N^{-0.75}$

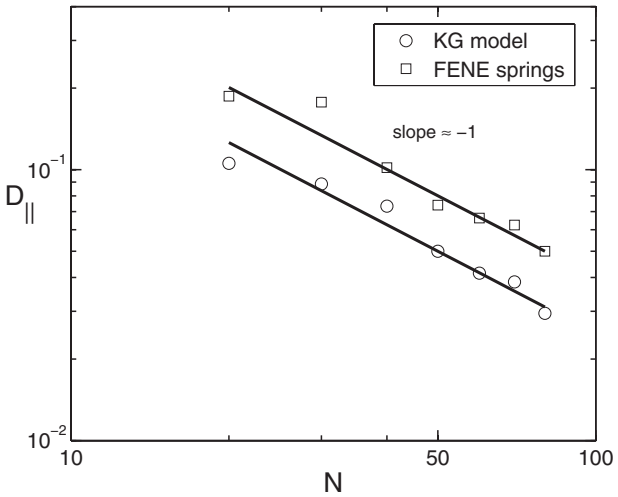

FIG. 3. Dependence of $D_\|$ on N near a chemically heterogeneous surface, when $\mathcal{A}=0.2$ and $q=1$, in the case of the KG model and FENE springs. The parameters used in the KG model are $b=4.67$ and $a=d_{ev}/2=0.72$. For FENE springs, we use $b=56.25$ and $a=d_{ev}/2=0.4$.

$=0.75$ if (i) the chain is stiff, (ii) the strength of HI is not weak, and (iii) the solvent is good. In contrast, ν is always 1 near a chemically heterogeneous surface. In experimental studies on DNA diffusion near lipid bilayers, $D_\| \sim N^{-1}$; our simulations for a chemically heterogeneous surface were able to reproduce this scaling. In experimental studies near physically heterogeneous solid surfaces, $D_\| \sim N^{-3/2}$ is observed and reptationlike arguments have been used to explain this scaling. However, our simulation model at present cannot be used to study diffusion near physically heterogeneous surfaces; this will be a subject of future investigation. It would also be useful to carry out simulations for larger values of N in order to determine whether the scaling exponents are different for sufficiently long chains. We expect that such simulations will enable the design of surface chemistry and topography to control the dynamics of confined polymers.

We thank Hongbo Ma and Professor Michael D. Graham of the University of Wisconsin-Madison for sharing their code for BD simulations of bead-spring chains that incorporates bead-wall HI. We are also grateful for resources from the University of Minnesota Supercomputing Institute and the U.S. Army Research Office.

[1] E. Sackmann, Science **271**, 43 (1996).
[2] B. Maier and J. O. Radler, Phys. Rev. Lett. **82**, 1911 (1999).
[3] B. Maier and J. O. Radler, Macromolecules **33**, 7185 (2000).
[4] L. Zhang and S. Granick, Proc. Natl. Acad. Sci. U.S.A. **102**, 9118 (2005).
[5] T. G. Desai, P. Keblinski, S. K. Kumar, and S. Granick, Phys. Rev. Lett. **98**, 218301 (2007).
[6] S. A. Sukhishvili, Y. Chen, J. D. Muller, E. Gratton, K. S. Schweizer, and S. Granick, Nature (London) **406**, 146 (2000).
[7] S. A. Sukhishvili, Y. Chen, J. D. Muller, E. Gratton, K. S. Schweizer, and S. Granick, Macromolecules **35**, 1776 (2002).
[8] S. R. Shannon and T. C. Choy, Phys. Rev. Lett. **79**, 1455 (1997).
[9] E. Falck, O. Punkkinen, I. Vattulainen, and T. Ala-Nissila, Phys. Rev. E **68**, 050102(R) (2003).
[10] R. Azuma and H. Takayama, J. Chem. Phys. **111**, 8666 (1999).
[11] T. G. Desai, P. Keblinski, S. K. Kumar, and S. Granick, J. Chem. Phys. **124**, 084904 (2006).
[12] H. J. Qian, L. J. Chen, Z. Y. Lu, and Z. S. Li, Phys. Rev. Lett. **99**, 068301 (2007).
[13] D. Mukherji, G. Bartels, and M. H. Muser, Phys. Rev. Lett. **100**, 068301 (2008).
[14] I. V. Pivkin and G. E. Karniadakis, J. Comput. Phys. **207**, 114 (2005).
[15] N. Hoda and S. Kumar, J. Chem. Phys. **127**, 234902 (2007).
[16] N. Hoda and S. Kumar, J. Chem. Phys. **128**, 164907 (2008).
[17] H. C. Öttinger, Phys. Rev. E **50**, 2696 (1994).
[18] H. C. Öttinger, *Stochastic Processes in Polymeric Fluids* (Springer, Berlin, 1996).
[19] R. M. Jendrejack, E. T. Dimalanta, D. C. Schwartz, M. D. Graham, and J. J. de Pablo, Phys. Rev. Lett. **91**, 038102 (2003).
[20] J. Rotne and S. Prager, J. Chem. Phys. **50**, 4831 (1969).
[21] H. Yamakawa, J. Chem. Phys. **53**, 436 (1970).
[22] K. Kremer and G. S. Grest, J. Chem. Phys. **92**, 5057 (1990).
[23] P. de Gennes, *Scaling Concepts in Polymer Physics* (Cornell University Press, Ithaca, 1985).
[24] R. G. Larson, *Constitutive Equations for Polymer Melts and Solutions* (Butterworths, Boston, 1988).
[25] R. B. Bird, C. F. Curtiss, R. C. Armstrong, and O. Hassager, *Dynamics of Polymeric Liquids* (Wiley, New York, 1987), Vol. 2.